Geochemistry Geophysics Geosystems G3

Article
Volume 13, Number 1
19 January 2012
Q01011, doi:10.1029/2011GC003787
ISSN: 1525-2027

Published by AGU and the Geochemical Society

Geophysical and geochemical survey of a large marine pockmark on the Malin Shelf, Ireland

M. T. Szpak
School of Chemical Sciences, Dublin City University, Glasnevin, Dublin 9, Ireland

X. Monteys
Geological Survey of Ireland, Beggars Bush, Haddington Road, Dublin 4, Ireland (xavier.monteys@gsi.ie)

S. O'Reilly
School of Chemical Sciences, Dublin City University, Glasnevin, Dublin 9, Ireland

A. J. Simpson
Department of Chemistry, Division of Physical and Environmental Science, University of Toronto at Scarborough, 1265 Military Trail, Toronto, Ontario M1C 1A4, Canada (andre.simpson@utoronto.ca)

X. Garcia
Geophysics Section, School of Cosmic Physics, Dublin Institute for Advanced Studies, Dublin 4, Ireland

Now at Unitat de Tecnologia Marina, CSIC, E-08003 Barcelona, Spain. (xgarcia@cmima.csic.es)

R. L. Evans
Department of Geology and Geophysics, Woods Hole Oceanographic Institute, 266 Woods Hole Road, Woods Hole, Massachusetts 02543, USA (revans@whoi.edu)

C. C. R. Allen
School of Biological Sciences, Queen's University Belfast, Medical Biology Centre, Lisburn Road, Belfast BT9 5AG, UK (c.allen@qub.ac.uk)

D. J. McNally and D. Courtier-Murias
Department of Chemistry, Division of Physical and Environmental Science, University of Toronto at Scarborough, 1265 Military Trail, Toronto, Ontario M1C 1A4, Canada

B. P. Kelleher
School of Chemical Sciences and Irish Separation Science Cluster, Dublin City University, Glasnevin, Dublin 9, Ireland (brian.kelleher@dcu.ie)

[1] Marine pockmarks are a specific type of seabed geological setting resembling craters or pits and are considered seabed surface expressions of fluid flow in the subsurface. A large composite pockmark on the Malin Shelf, off the northern coast of Ireland was surveyed and ground truthed to assess its activity and investigate fluid related processes in the subsurface. Geophysical (including acoustic and electromagnetic) data confirmed the subsurface presence of signatures typical of fluids within the sediment. Shallow seismic profiling revealed a large shallow gas pocket and typical gas related indicators such as acoustic blanking and enhanced reflectors present underneath and around the large pockmark. Sulphate profiles indicate that gas from the shallow reservoir has been migrating upwards, at least recently. However, there are no chimney structures

observed in the sub-bottom data and the migration pathways are not apparent. Electromagnetic data show slightly elevated electrical conductivity on the edges of the pockmarks and a drop below regional levels within the confines of the pockmark, suggesting changes in physical properties of the sediment. Nuclear Magnetic Resonance (NMR) experiments were employed to characterize the organic component of sediments from selected depths. Very strong microbial signatures were evident in all NMR spectra but microbes outside the pockmark appear to be much more active than inside. These observations coincide with spikes in conductivity and the lateral gas bearing body suggesting that there is an increase in microbial activity and biomass when gas is present.

Components: 10,100 words, 9 figures, 2 tables.

Keywords: Malin Shelf; NMR; electromagnetic; microbial; organic matter; pockmark.

Index Terms: 4273 Oceanography: General: Physical and biogeochemical interactions.

Received 8 July 2011; **Revised** 4 November 2011; **Accepted** 17 November 2011; **Published** 19 January 2012.

Szpak, M. T., X. Monteys, S. O'Reilly, A. J. Simpson, X. Garcia, R. L. Evans, C. C. R. Allen, D. J. McNally, D. Courtier-Murias, and B. P. Kelleher (2012), Geophysical and geochemical survey of a large marine pockmark on the Malin Shelf, Ireland, *Geochem. Geophys. Geosyst.*, *13*, Q01011, doi:10.1029/2011GC003787.

1. Introduction

[2] Pockmarks are a specific type of geological setting resembling craters or pits. They are predominantly found in soft, fine-grained seafloor surfaces [*Hovland and Judd*, 1988] but also have been discovered in other aquatic environments including lakes, deltas and estuaries [*MacDonald et al.*, 1994; *Berkson and Clay*, 1973; *Hovland et al.*, 1997]. Pockmarks are usually sub-circular but can be elongated by currents to resemble ellipsoidal craters [*Bøe et al.*, 1998] or composite when two or more pockmarks merge [*Stoker*, 1981]. Asymmetric, elongated and trough-like pockmarks have also been reported [*Hovland and Judd*, 1988]. They can be found isolated, occurring in groups referred to as "pockmark fields" [*Fader*, 1991; *Kelley et al.*, 1994] or as large chains of craters known as "pockmark trains" [*Pilcher and Argent*, 2007]. Although it is still debated, marine pockmark formation is generally associated with upward fluid migration through the seabed. In most pockmark studies this fluid has been found to be hydrocarbon gas and therefore pockmarks are commonly referred to as gas escape features [*Judd and Hovland*, 2007]. From a global point of view, as pockmarks comprise one of the geomorphological indications of fluid flow, and gas flow in particular, they may be considered contributors to the global methane and carbon cycles. Although no attempt has been made to estimate their input into carbon cycling models, *Judd and Hovland* [2007] argue that seepage contribution might require methane flux revisions. Pockmarks and seepages are often linked with an increased abundance and diversity of life across all trophic levels. It has been reported that in sites with documented gas accumulations and active gas migration microbial activity is intensified and often bacterial based food webs are present [*Dando et al.*, 1991]. Increased rates of processes such as anaerobic oxidation of methane (AOM), sulphate reduction, and sulphide oxidation have also been reported [*Boetius et al.*, 2000; *Pimenov et al.*, 2000].

[3] The Malin Deep Pockmark Field lies on the Irish continental shelf, approximately 70 km offshore northwest Ireland (Figure 1). The area lies in a complex structural setting, delimited to the North by the Stanton Banks Fault and to the south by the Malin Terrace [*Dobson and Whittington*, 1992]. The Skerryvore Fault (SKF), a major normal fault, divides the study area into two different basins, the Donegal Basin and the West Malin Basin (Figure 1). The Donegal Basin extends parallel to the north coast of Ireland into the area of the Malin Sea with an east-northeast trend. It consists of two different sub-basins. The North Donegal Basin, which is of Paleozoic age, lies to the northwest of the SKF. To the south lies the Donegal Basin, comprised of Permo-Triassic to Jurassic units. West of the SKF, the Malin Basin is dominated by three separate faulted synclines, the Skerrivore Trough, the Malin Trough and the half-graben formed from the western extension of the Colonsay Basin. Two structural trends, one NE-SW (Caledonian) and another almost

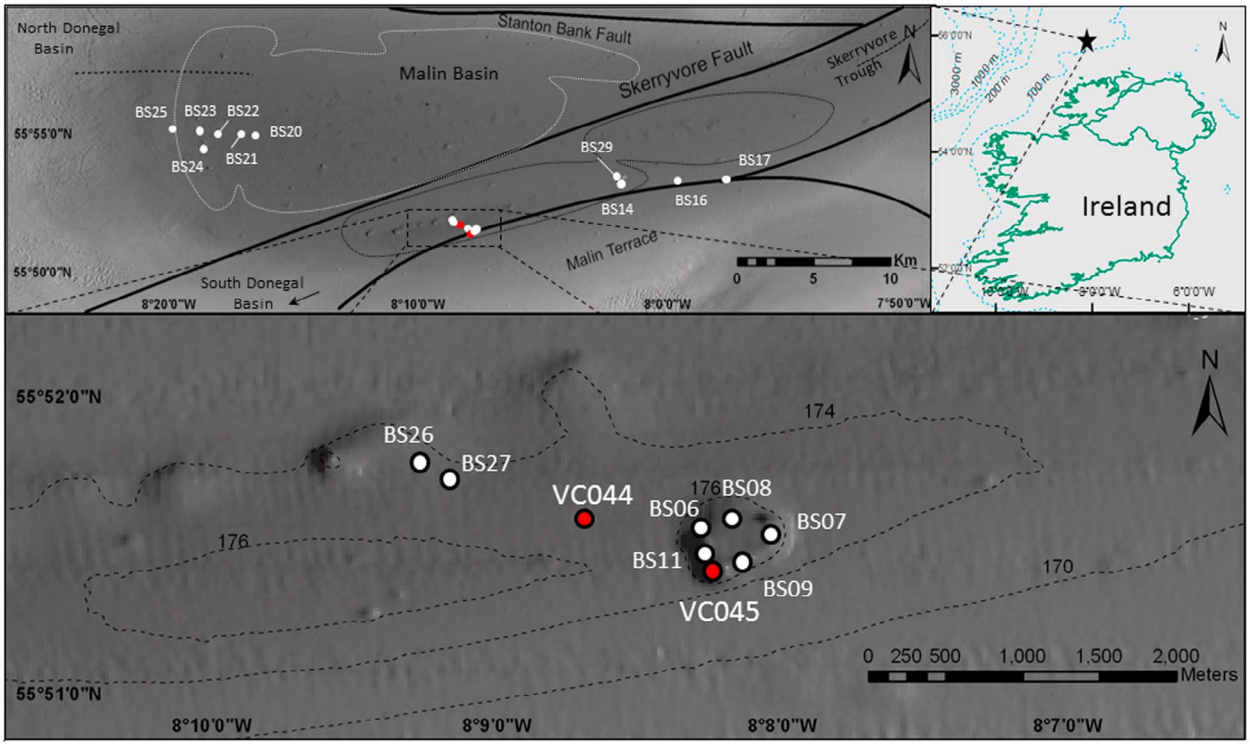

Figure 1. Multibeam shaded relief bathymetry with major structural features: Skerryvore Fault (SKF) and Stanton Bank Fault (SBF) and (top) index map with site location. Despite large scale of the map linear pockmark clusters are clearly visible in the Malin Deep micro basin south of SKF here marked a with black dotted line. Several minor unit pockmarks are visible in the Malin Deep area marked with a dotted light gray line. (bottom) Detailed sampling site map shows structural details of targeted composite pockmark.

orthogonal NNW-SSE (Paleozoic) dominate the region. Faults in a NNW-SSE direction, developed across this region in a dextral strike-slip stress regime. It induced late Carboniferous (Variscan) compressional stresses and later extensional episodes in the early Mesozoic (orthogonal to the basin bounding faults) are likely to have reactivated Caledonoid thrusts, generating a series of half-grabens and late Paleozoic to early Mesozoic basins. Igneous intrusions are common across the Malin Shelf including centers such as the Malin Complex [*Riddihough*, 1968] and minor bodies on the Malin Trough closer to the study area. Quaternary sediments are recorded throughout the Malin Sea area, with thicknesses varying from north to south from 175 to 125 m [*Evans et al.*, 1986].

[4] Overall, the Malin Sea seafloor is characterized by complex seabed geology with a variety of sediment facies, including recent sand bed forms, gravel lags and coarser clasts ranging in size from pebbles to boulders. However, the basin floor around the pockmark field is characterized by a smooth and soft seabed composed of fine-grained marine sediments, ranging from fine sands to silts. The seabed in the study area contains more than 220 gas related pockmarks distributed in clusters primarily around the main structural lineaments [*Monteys et al.*, 2008a]. Large composite pockmarks are predominantly found in a micro-basin south of SKF (Figure 1).

[5] Hydrocarbons have been encountered in several of the northwest offshore basins, particularly as with thicker permotriassic sequences. Hydrocarbon prospects rely on the existence of carboniferous source rocks, however, Jurassic to Cretaceous source rocks have also been documented in the region. Palaeogene reactivation of fractures may have allowed the leakage of reservoired hydrocarbons to the upper subsurface [*Parnell*, 1992].

[6] Here, we report geophysical characteristics and couple this information with geochemical and bulk organic matter characteristics of sediment from six meter cores collected within and outside a pockmark located on the Malin Deep Pockmark Field. The goal was to determine whether physical and chemical properties differ inside and outside a pockmark and

whether these properties can help elucidate formation mechanisms.

2. Materials and Methods

2.1. Bathymetry

[7] Bathymetry data were collected in 2003 and 2006 as part of the INSS (Irish National Seabed Survey) and its successor, the INFOMAR (Integrated Mapping for the Sustainable Development of Ireland's Marine Resources) program [*Dorschel et al.*, 2010]. Data were acquired onboard the R.V. Celtic Explorer and R.V. Celtic Voyager using a Kongsberg-Simrad EM1002 multibeam echosounder, with an operational frequency of 93–98 kHz and pulse length of 0.7 ms and low survey speed (2–3 knots). Resulting bathymetric terrain models were gridded at 5 × 5 m. High resolution bathymetry was crucial in identifying smaller gas escape features [*Monteys et al.*, 2008a].

2.2. Sub-bottom Profiler

[8] Sub-bottom profile data were acquired using a heave-corrected SES Probe 5000 3.5 kHz transceiver in conjunction with a hull-mounted 4° × 4° transducer array. Acquisition parameters, data logging and interpretation were carried out using the CODA Geokit suite. Both Raw Navigation string and Heave Compensation string are fed into the Coda DA200 system (from the Seapath 200). An average estimated acoustic velocity of 1650 m/s was used to calculate the thickness of the sedimentary units. Acoustic penetration in some areas was in the order of 60 m below seabed with approximately 0.4 m vertical resolution.

2.3. Towed Electromagnetic Data

[9] The towed-electromagnetic (EM) system discussed in this paper consists of a ~40 m-long array, which is towed in contact with the seafloor at speeds of 1–2 knots. The EM transmitter, a horizontal magnetic dipole, generates harmonic magnetic fields over a range of frequencies (~200 Hz–200 kHz), and the three receivers, tuned to measure these magnetic fields, are towed at fixed distances behind (4 m, 12.6 m and 40 m) and provide average conductivities over seafloor depths roughly one-half the source-receiver offset (i.e., ~2 m, 6 m and 20 m below seafloor respectively). At a given frequency the strength of magnetic fields decays away from the transmitter as a function of the conductivity of the seafloor (i.e., according to the skin depth), decaying more rapidly in more conductive media. Measurements are made roughly every 10 m along the towline, so sensitivity to lateral variations in structure is high. Each receiver measures data at 3 distinct frequencies [*Evans*, 2007] and in general the information from the 6 pieces of information (3 amplitudes and 3 phases) on each receiver are combined into a single apparent resistivity measurement - the resistivity of the uniform seafloor that best matches the observations. The frequencies are chosen based on skin-depths between the transmitter and receiver for a range of likely seafloor conductivities. That is, the highest frequency is appropriate for a highly resistive seafloor while the lowest frequency is appropriate in the case where the seafloor is quite conductive, the higher frequency fields in this case having been more attenuated. It is therefore possible, and sometimes desirable, to examine single frequency data, using the most appropriate frequency based on the observed conductivities. In Figure 2 we have converted amplitude data from one of the frequencies on the 13m receiver to an apparent conductivity.

[10] The sensitivity of the magnetic dipole-dipole system, along with the physics of the propagation of the fields through the seafloor was presented by *Cheesman* [1989]. Further details of the system are given by *Evans* [2007]. The system has been used previously across an area of gas discharge in the Gulf of Mexico [*Ellis et al.*, 2008]. In this instance, extremely high conductivities within the subsurface were observed, resulting from the advection of warm briny fluids from depth toward the seafloor. This response was the opposite expected for a gas rich sub seafloor, for which conductivity should decrease. In this paper we focus on the electromagnetic data for the first 6 m of the seabed, full discussion of the EM data is published elsewhere [*Garcia et al.*, 2007].

2.4. Sediment Samples

[11] Sediment vibrocores, VC044 (outside pockmark) and VC045 (inside pockmark) were collected during the 2008 RV Celtic Explorer (CE08) expedition. Core locations and lengths are shown in Table 1. Cores were cut into sections and wax-sealed. Cores were 140 mm in diameter. The cores were refrigerated for the duration of the cruise and afterwards scanned for physical properties on a MultiSensor Core Logger (Geotek, United Kingdom) sub-sampled and frozen. Additionally several grab samples were collected across the basin to characterize surface sediments.

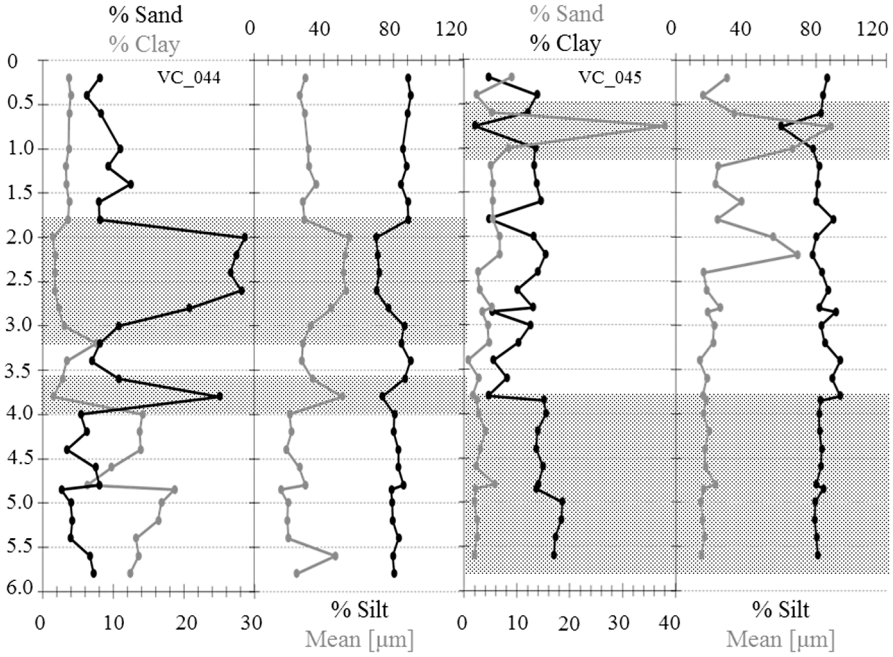

Figure 2. Grain size distribution of the pockmark (VC045) and the reference core (VC044). Shaded areas denote specific facies discussed in the text.

2.5. Bulk Parameters

[12] Sediment samples from both cores were sized with a Mastersizer S laser granulometer (Malvern Ltd, United Kingdom) after dry sieving analysis and chemical disagglomeration with sodium pyrophosphate ($Na_4P_2O_7 \bullet 10\ H_2O$). The data was processed with the Gradistat software package [*Blott and Pye*, 2001].

[13] Total organic carbon (TOC) analysis was performed by the combustion method according to standard protocol. Briefly, samples were treated with 1 N HCl prior to the analysis to remove inorganic carbonates, oven-dried at 70°C, combusted at 960°C and analyzed with a Vario EL elemental analyzer (Elementar GmbH, Germany). Additionally, thermo-gravimetric analysis was performed on larger aliquots at 500°C for 24 h.

[14] Pore water for sulphate and chloride analysis was extracted by centrifugation. Sulphate and chloride concentrations were determined by ion chromatography (IC) according to standard methodology. Sulphate flux was calculated according to Fick's first law of diffusion and corrected for sediment tortuosity as suggested by *Schulz and Zabel* [2006]. Calculations were based on sulphate diffusion coefficient in seawater at 5°C (5.72×10^{-10} m^2 s^{-1} [*Boudreau*, 1997], tortuosity derived from electrical conductivity [*Boudreau*, 1997]; θ^2 is 2.19 and 2.05 for the VC044 and VC045 respectively) and sediment porosity (mean derived from gamma ray attenuation measurements from top of both cores to SMTZ; Φ is 0.55 and 0.59 for the VC044 and VC045 respectively).

2.6. Isolation of Sediment Organic Matter

[15] The sediment organic matter (SOM) extracts were prepared by exhaustive extraction (0.1 M NaOH), filtration [0.22 μm polyvinylidene fluoride (PVDF)], cation-exchange (Amberlite 1200+ resin), and freeze–drying. Sediment samples were pretreated with hydrofluoric acid (HF) to reduce paramagnetic species according to the method of *Gonçalves et al.* [2003]. Note that very little if any loss of color was observed during HF treatment. Investigations in our laboratory (data not shown)

Table 1. Core Locations and Lengths

Core	Water Depth (m)	Latitude (°N)	Longitude (°E)	Core Length (m)
VC_044	175	55.85980	−8.14500	5.80
VC_045	180	55.85680	−8.13720	5.90

Table 2. Grain Size Distribution and TOC for Surface Sediment Samples Shown in Figure 1

Sample	Mean (μm)	Sorting (σ)	Composition					Textural Group	TOC (%)
			% Clay < 2 μm	% Silt 2–63 μm	% Mud	% Sand 63–880 μm	% Shell		
BS25	134.9	2.378	6.3	29.6	35.9	64.1	0.0	Muddy Sand	<0.2
BS23	114.1	2.230	6.0	33.8	39.7	60.3	0.0	Muddy Sand	0.3
BS24	95.0	2.268	6.9	40.8	47.7	52.3	0.0	Muddy Sand	0.2
BS22	81.4	1.921	5.2	47.7	52.9	46.4	0.0	Muddy Sand	0.5
BS21	130.9	2.097	4.6	31.8	36.4	63.1	0.5	Muddy Sand	-
BS20	66.1	2.236	8.8	53.1	61.9	38.1	0.0	Sandy Mud	0.4
BS26	69.4	2.131	7.4	52.2	59.6	40.4	0.0	Muddy Sand	-
BS27	67.4	2.075	7.1	53.5	60.6	39.4	0.0	Sandy Mud	0.4
BS07	58.5	2.139	8.4	59.0	67.5	32.5	0.0	Sandy Mud	0.5
VC044	29.2	1.562	3.7	88.3	92.0	8.0	0.0	Mud	-
BS09	58.3	2.157	8.5	59.2	67.8	32.2	0.0	Sandy Mud	0.4
BS11	62.8	2.119	8.0	55.7	63.6	36.4	0.0	Sandy Mud	0.3
VC045	28.9	1.704	4.6	86.4	91.0	9.0	0.0	Mud	-
BS06	48.3	2.229	10.4	67.3	77.7	22.3	0.0	Sandy Mud	-
BS08	57.7	2.114	8.5	61.7	70.2	29.8	0.0	Sandy Mud	-
BS14	65.7	2.353	10.0	56.4	66.4	32.9	0.7	Sandy Mud	-
BS29	60.1	1.952	6.6	61.5	68.1	31.9	0.0	Sandy Mud	-
BS16	48.0	2.226	10.4	64.7	75.1	21.9	2.9	Sandy Mud	-
BS17	71.2	2.140	7.3	50.8	58.1	40.4	1.5	Muddy Sand	-

and those by others [*Gonçalves et al.*, 2003; *Gélinas et al.*, 2001] indicate that the 1D NMR spectra before and after HF treatment are very similar; however, the treatment permits higher-quality 2D NMR to be obtained.

2.7. Nuclear Magnetic Resonance (NMR) Analysis

[16] Each sample (~40 mg) was re-suspended in 1 mL of deuterium oxide (D_2O) and titrated to pH 13 using NaOD (40% by weight) to ensure complete solubility. Samples were analyzed using a Bruker Avance 500 MHz NMR spectrometer equipped with a ^{1}H-^{19}F-^{13}C-^{15}N 5 mm, quadruple resonance inverse probe (QXI) fitted with an actively shielded Z gradient. 1-D solution state ^{1}H NMR experiments were performed at a temperature of 298 K with 128 scans, a recycle delay of 3 s, 16384 time domain points, and an acquisition time of 0.8 s. Solvent suppression was achieved by presaturation utilizing relaxation gradients and echoes [*Simpson and Brown*, 2005]. Spectra were apodized through multiplication with an exponential decay corresponding to 1 Hz line broadening, and a zero filling factor of 2. Diffusion-edited (DE) experiments were performed using a bipolar pulse longitudinal encode-decode sequence [*Wu et al.*, 1995]. Scans (1024) were collected using a 1.25 ms, 52.5 gauss/cm, sine-shaped gradient pulse, a diffusion time of 100 ms, 16384 time domain points and 819 ms acquisition time. Spectra were apodized through multiplication with an exponential decay corresponding to 10 Hz line broadening and zero filling factor of 2.

[17] Heteronuclear Multiple Quantum Coherence (HMQC) spectra were obtained in phase sensitive mode using Echo/Antiecho gradient selection. The HMQC experiments were carried out using 256 scans with 128 time domain points in the F1 dimension and 1024 time domain points in the F2 dimension. A relaxation delay of 1 s and ^{1}J ^{1}H-^{13}C of 145 Hz were used. F2 dimensions in HMQC experiments were processed using an exponential function corresponding to a 15 Hz line broadening. The F1 dimension was processed using a sine-squared function with a $\pi/2$ phase shift and a zero-filling factor of 2.

3. Results and Discussion

3.1. Characterization of the Malin Deep Sediments

[18] The Malin basin is a setting with a predominance of fine-grained sediment cover and occasional gravel patches and sand ribbons particularly to the northwestern part of the basin (Figure 1). Recent seabed sampling and historical published maps have shown that around the center and deepest part of the basin (known as Malin Deep) is composed primarily of silts, with a variable fine sand fraction (Table 2). Toward the edges of the basin, the sediment becomes gradually slightly sandier. This interpretation of the regional sediment composition is in concordance

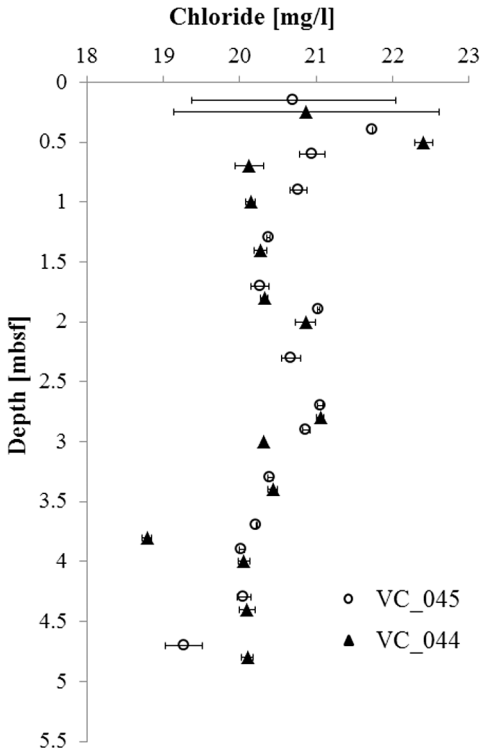

Figure 3. Chloride concentrations versus depth in the pockmark (VC045) and the reference (VC044) core. Error bars are standard error (σ) values.

with the acoustic seabed classification model for the area developed by the Geological Survey of Ireland [*Monteys et al.*, 2008b]. According to *Dunlop et al.* [2010] the western boundary of the Malin Shelf was under the influence of main ice streamflow lines and frequently scoured by detached icebergs. The Barra and Donegal sediment fans are a possible source of the glaciomarine sediment deposits in this shelf area. Seabed sediment maps from the pockmark region published by the British Geological Survey [*Evans et al.*, 1986], and additional bottom sediment samples presented in this study show a near-seabed composition of marine fine shelly sediments, ranging in grain size from muddy sand to sand. The average mean grain size of the surface sediments varies from 60.5 μm (n = 9) in the center of the basin to 111.3 μm (n = 5) in the western boundary and 71.2 μm (BS17). The thickness of this surface unit varies from 0.1 to 0.5 m (BS16 and BS17) and 0.3–0.75 m (BS22 and BS21) in the eastern and western location respectively (data not shown). In the area of the composite pockmark the surface layer was thinner and ranged from 0.1 to 0.3 m (BS06 and BS08). The mean grain size of the sediment inside of some pockmark units (e.g., BS06, BS07) is slightly lower than surrounding sediments which suggest that some of the craters act as sinks for the finest grains.

[19] The reference core (VC044) shows a sand unit between 2.0 and 3.0 mbsf. This unit is correlated with the prominent enhanced reflector (ER) observed in sub bottom data (Figure 2) and a decrease in porosity (data not shown). The uppermost 1.5 m of the reference core shows slightly higher mean grain size than the pockmark core (29.9 μm, n = 12; 23.9 μm, n = 17 respectively), indicating that more fine-grained material is buried within the pockmark than outside. In the lower section of both cores (4–6 mbsf) a notable increase in clay content is observed, however, the clay content in the pockmark core is on average higher than in the reference core, particularly in the upper section of the core (12.1% compared to 3.1% respectively). The sedimentary patterns in the pockmark core (VC044) appear structureless, homogenous and with less clear lamination than in the reference core (VC045). This could be indicative of sediment movement, a reminiscence of a violent pockmark formation [*Judd and Hovland*, 2007].

3.2. Evidence of Gas in the Sediment

[20] Pockmarks are considered surface expressions of seabed fluid expulsion. Although the exact formation mechanisms remain elusive, three types of formation fluids are thought to be responsible for formation of most pockmarks: groundwater springs, hydrocarbon gas and hydrothermal gas [*Judd and Hovland*, 2007]. Active groundwater discharges can be identified acoustically [*Hay*, 1984] or by seawater conductivity changes near the seepage [*Christodoulou et al.*, 2003]. The Malin Deep remains separated from aquifer influence by the Malin Terrace bedrock with very low hydraulic conductivity [*Dobson and Whittington*, 1992]. There is also no evidence of groundwater discharge from historical and more recent oceanographic surveys [*Gowen et al.*, 1998; *Monteys et al.*, 2008a]. Detection of past and periodic events however require seabed sampling as only changes in pore water chemistry can show evidence of freshwater influence. In the studied setting, chloride concentrations were typical for marine environments and have shown little variability down the cores (Figure 3). There we also no significant differences between pockmark core and reference core with chloride concentrations being moderately positively correlated (R^2 = 0.46). However, hydroacoustic surveys have revealed a presence of shallow gas throughout the entire Malin Deep area [*Garcia et al.*,

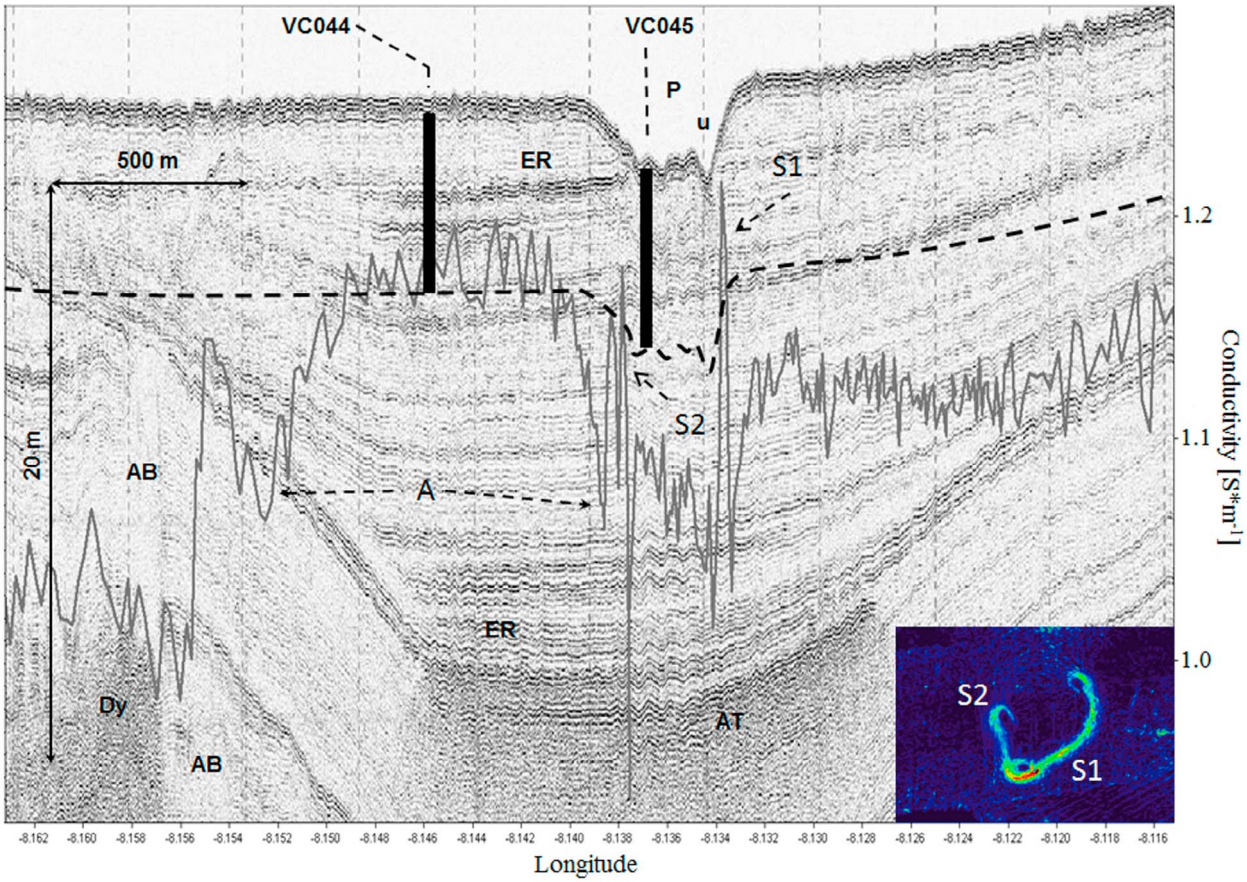

Figure 4. Sub-bottom 3.5 kHz profile (pinger) of the composite pockmark (P) in the Malin Deep microbasin with one of the pockmark units (u) visible. The pockmark is 750 m wide (measured from opposing ends) with three sub-circular units approximately 50 m wide and 8.5 m deep. Overlayed gray line shows conductivity measurements derived from towed EM system and the dashed black line denotes the depth range for the system. High conductivity values present in both sides of the pockmark (S1 and S2) are associated with disturbed sediment on the edges of the unit pockmarks. The largest conductivity anomaly (A) correlates accurately with the extent of the strong reflector in the sub bottom record associated to gas facies and cannot be explained by changes in sediment structure. Gas enhanced reflectors (ER), acoustic turbidity (AT) and numerous vertical acoustic blanking (AB) signals particularly in the vicinity of igneous body (Dy) are clearly visible. Although the identity of Dy is not obvious from the pinger data shown here, the total intensity magnetic data, sparker and 2D seismic data confirmed its identity, geometry, spatial distribution and intrusive character (data not shown; Geological Survey of Ireland, 2003). Vertical bold lines depict approximated locations of two 6 m long vibrocores collected at the site, length of the lines is to scale.

2007]. Most of the features in the Malin Deep area are sub-circular unit pockmarks scattered across the 23000 km^2 of seabed. Moreover in the micro-basin on the southern boundary of the Malin Deep (Figure 1) there are several composite features created by repeating venting events. This might indicate that fluids underneath these features reach the seabed more frequently than in other places. Profiler data clearly illustrates a visible gas pocket underneath the composite pockmark studied here (Figure 4).

[21] Multiple gas enhanced reflectors (ER) are observed above the gas pocket just above the gas front characterized by visible acoustic turbidity (AT) followed by acoustic blanking (AB) due to a decrease in the backscatter of the acoustic signal (Figure 4). These signals mark the impermeable boundary of this shallow gas accumulation. Just above the gas front more discrete, ERs are visible possibly indicating gradual upward migration of gas and accumulation in more gas permeable, coarser sediment layers such as sand lenses or gravel patches. Similar signals are present west of the pockmark where particle size and logging data from vibrocore VC044 confirmed the presence of sandy layers that coincide with the observed lateral ER (Figures 2 and 4). Interestingly, during the on-deck

sample processing, vigorous degassing was documented at the reference core in two of the sections but regrettably, volatiles sampling was not possible during the cruise. Since initial pockmark formation through an undisturbed seabed is believed to have a violent, blow-out like characteristic, subsequent fluid migration is likely to utilize already established pathways including temporary reservoirs [*Judd and Hovland*, 2007]. However, more recent studies [e.g., *Hovland et al.*, 2010] suggest that gentle venting events might occur periodically outside of main pockmark feature when the gas supply from the reservoir is low. The 'gas piston' will act as hydraulic pump causing pore water expulsion on the surface. The eruption of the gas can only occur when the fluid in the reservoir is over-pressured enough to force its way through the original seal. Directly underneath the pockmark (P) featureless, mixed sediment is visible, possibly a remnant of pockmark formation, contrary to clear lamination that is visible in sediments in the vicinity of this feature. Moreover, numerous occurrences of vertical acoustic blanking (AB) are present in the surrounding sediments. The exact meaning of vertical AB is still poorly understood and widely debated [*Judd and Hovland*, 2007]. These signals are likely to be indicative of active fluid migration or fluid related sediment structure alteration, particularly with other evidence of fluid in the subsurface. However, acoustic signal effects such as signal starvation or amplitude blanking cannot be ruled out [*Judd and Hovland*, 2007]. Interestingly though, these signals are clearly more abundant above and in the vicinity of igneous intrusions (Dy) which are commonly associated with fluid migration pathways [*Khilyuk et al.*, 2000].

[22] Based on the marine electromagnetic plot crossing the pockmark region and imaging approximately the upper 6 m below seafloor, conductivity measurements are significantly affected by shallow gas pockets and/or gas disturbed sediments (Figure 4). The presence of gas and changes in sediment porosity is expected to modify the conductivity of the seafloor. Gas within the sediment framework will act as an electrical insulator, potentially decreasing conductivity by several orders of magnitude. However, the degree to which the bulk conductivity will be modified by the gas phase depends on several parameters including the gas concentration and how it is distributed between grains [*Evans*, 2007]. In general, the extent of the gas pocket, as recorded in the sub-bottom profiles, falls in an area of lowered and more irregular conductivity values (and is likely to be the dominant factor responsible for the conductivity minimum in this area indicating migration of gas to the seabed from the underlying gas reservoir).

[23] We observe a relative increase in the electrical conductivity on the edges of the unit pockmarks (S1 and S2), and a drop below regional levels within the pockmark. These conductivity spikes are unusual and surprisingly correlated with the pockmark edges. Similar signals were also observed in another large pockmark in this area. Angle variation between receiver and transmitter caused by seabed roughness could produce an artificial signal, however, seabed slopes on S1 and S2 are low (<5°) and the soft sediments did not offer additional resistance to the towed instrument. It is therefore unlikely that S1 and S2 are EM system related artifacts. Alternatively, these spikes could coincide with shallow subsurface features of the pockmark, such as cracks or fractures, that could be utilized as migration pathway and accumulate pore fluids as described by *Cathles et al.* [2010] and *Judd and Hovland* [2007]. Flow obstacles such as methane-derived authigenic carbonates (MDACs) can force alternative migration pathways and result in local pore fluid overpressure including pockmark walls in some scenarios [*Hovland et al.*, 2010]. Low-permeability, fine-grained sediments can act as flow obstacles in a similar manner. Although fluid migration pathways are not clearly defined in the shallow seismic record, the lateral gas related enhanced reflectors indicate that fluid displacement might contribute to the increased conductivities observed at the edges of the pockmark.

[24] More important to note, is a significant conductivity increase (A) extending over 500 m west of the pockmark associated to a near-surface (ca. 3 mbsf) gas related enhanced reflector (Figure 4). This anomaly is opposite to the expected response (decrease). The ER reflector coincides with a lithostratigraphic unit in the sediment core, characterized primarily by coarser sediment grain size (VC044, 2–4 mbsf; Figure 2), as well as prominent microbial signatures observed in the NMR spectra (see 3.5). Interestingly, *Atekwana et al.* [2004] and *Allen et al.* [2007] reported that higher bulk conductivities in sediments are associated with microbial activity stimulated by the presence of petroleum hydrocarbons. They found a higher percentage of hydrocarbon degrading microbial populations in sediment characterized by increased bulk conductivity and showed that the higher conductivity may result from increased fluid conductivity related to microbial degradation. Furthermore, *Abdel Aal et al.* [2010a] demonstrated in a controlled environment

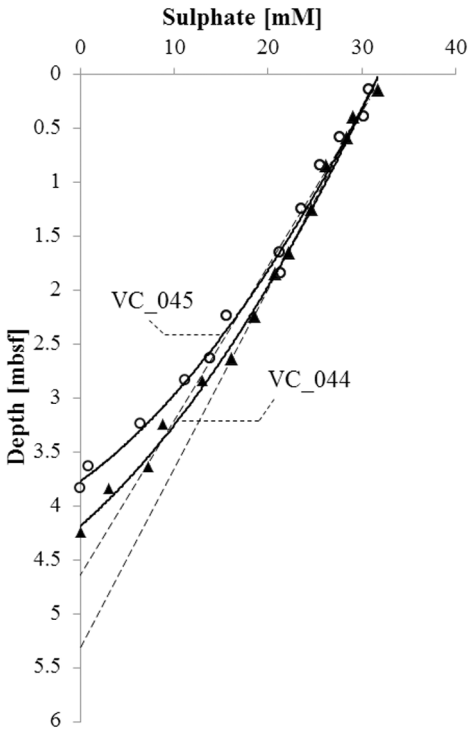

Figure 5. Sulphate concentration versus depth for the pockmark (VC045) and the reference (VC044) cores. Black curves are second order polynomial fits showing nonlinear concentration change with depth indicating flux variation. The dashed line depict linear sulphate gradient observed in the first 3 mbsf and the predicted SMTZ depths should the sulphate depletion rate have stayed constant.

that exopolymeric substances produced by microcolonies and adhered to grains, increased the conductivity of the system. *Abdel Aal et al.* [2010b] also show that specifically, live microbial biomass increased the conductivity of the system while the presence of dead cells resulted in considerably smaller responses. Since migration of light hydrocarbon gas is observed in the Malin Shelf sediments, we suggest that changes in microbial population and their activities contribute to higher conductivity signals such as the discrete conductivity anomaly (A).

3.3. Origin of the Shallow Gas

[25] The origin of this shallow gas remains unclear although deep structural features of this setting suggest a deep source. The pockmark spatial distribution is axially correlated with primary (Skerryvore Fault and Stanton Bank Fault) and secondary faults and folds. Fluid accumulation facies are present at the base of post glacial, fine-grained Jura formation with evidence of possible lateral migration toward the center of the basin. Historical sub-bottom data suggests that Paleogene igneous intrusions indeed act as natural obstacles for stratified diffusive fluid migration and might contribute to numerous gas accumulations by channeling and focusing fluid into shallow pockets [*Monteys et al.*, 2008b]. The Malin Deep is a setting with thick fine-grained sediment cover and quite high sedimentation rates ranging from 30 cm/ky to over 130 cm/ky in the last 5 ky [*Monteys et al.*, 2008b]. With sufficient flux of organic carbon to the seabed these sedimentological conditions would have favored shallow anoxia and intensive microbial methanogenesis [*Stein*, 1990]. However, the organic carbon content of the Malin Deep surface sediments does not exceed 0.5% (mean 0.35%, n = 9, Table 2) and with only a fraction of that reaching the methanic zone it appears that without a deep, rich in organic carbon source rock microbial methanogenesis is likely to be a contributor rather than the dominant source of the Malin Deep gas.

3.4. Pockmark Activity

[26] Intensive video surveying was carried out to assess the activity and surface topography of the studied pockmark. We did not record any hard ground outcrops (MDACs), bacterial mats, increased macrofauna accumulation or obvious seepage in any of the video lines despite several crossings of all of the pockmark sub-units. The pockmark's seabed topography did not differ from that of the surrounding seabed. Video data clearly suggest that this pockmark remains dormant and fluid activity is confined to the sub-surface sediments as visualized by the sub-bottom data (see 3.3 and Figure 4). Interestingly, pore water sulphate profiles from both cores show a slight concave up curvature (Figure 5). Both profiles show a clear linear gradient to around 2.7 mbsf with the pockmark core showing a slightly higher rate of sulphate consumption than in the reference core (6.6 mmol/m^3m and 6.0 mmol/m^3m respectively). From around 3.2 mbsf new steeper gradient was observed in both cores indicating more rapid sulphate removal than expected in a stead state scenario. Similarly, the pockmark core gradient is higher than the one in the reference core (12.0 mmol/m^3m and 9.4 mmol/m^3m respectively). According to *Niewöhner et al* [1998] and *Borowski et al.* [1996] rapid change in depositional conditions and/or upward methane flux, control the shape of the sulphate profiles in settings with a high methane flux derived from intensive methanogenesis as well as deeper sources. In a steady state situation sulphate

profiles are straightened out by intensive anaerobic oxidation of methane (AOM) fueled by methane migrating toward the surface. Although oxidation of organic carbon also plays a role in sulphate reduction the rate of these processes favor more rapid AOM which effectively controls the sulphate profile shape. High sulphate reduction rates and availability of readily degradable organic matter are crucial in low methane flux scenarios as shown by *Ferdelman et al.* [1999]. *Hensen et al.* [2003] on the other hand, demonstrated that recent changes in methane flux will affect the sulphate profile curve. In the case of decreased flux a concave down profile is expected, with consumption of sulphate by degradation of organic matter being the controlling process. Increased flux will cause a concave up sulphate profile as was the case with both cores studied here. Kink type profiles can over time be transformed into concave up profile. The kink profile origin is uncertain and it is possible that they can form in more than one scenario. *Zabel and Schulz* [2001] postulated sedimentary slide, *Fossing et al.* [2000] suggested non-local transport mechanism such as irrigation of bubble ebullition and *Schulz et al.* [1994] proposed sulphide re-oxidation via Fe-hydroxides. *Hensen et al.* [2003] argue that they are short-lived phenomenon and represent a transient state that is smoothed out after the event took place by the dominant controlling processes rapidly. In the context of the studied pockmark, Malin Deep changes in sulphate profiles might indicate that methane from the shallow reservoir (Figure 4) was migrating upwards and influencing microbial processes in the first few meters of the seafloor and the sulphate-methane transition zone (SMTZ) in particular. Additionally, the flux intensity varies between the pockmark and the reference core. Both profiles show evidence of an increased upward methane flux but in the reference core the flux is 25% lower (3.2 mmol CH_4 m^{-1} yr^{-1}) than directly above the reservoir (4.3 mmol CH_4 m^{-1} yr^{-1}) and results in a deeper SMTZ (4.2 mbsf and 3.8 mbsf respectively).

3.5. Organic Matter and Microbial Activity in Gas Charged Sediments

[27] NMR spectra were acquired for alkaline organic extracts from six depths from both the inside and outside core. The spectra for depths of 3 and 5 mbsf within the pockmark (data not shown) were very broad even after repeated analysis. This may be due to a high concentration of magnetic species present in these fractions within the pockmark as this problem was not encountered outside [*Pake and Estle*, 1973; *Simpson et al.*, 2006]. We therefore only compare samples taken from depths of 0, 2, 4 and 5.7 mbsf.

[28] Figure 6 displays the ^{1}H NMR spectra from different core depths inside and outside the pockmark. The ^{1}H NMR spectra were sub-divided into two separate regions (0–6 ppm in Figure 6) so as to better highlight compositional differences. Microbial cells appear to be in abundance, as indicated by the very intense signal from peptidoglycan at 2.03 ppm (*N*-acetyl functional group) which is a major component in bacterial cell walls [*Simpson et al.*, 2007b]. However, this peak cannot be assigned with certainty from the ^{1}H NMR spectra alone. Alternatively, HMQC NMR spectroscopy provides ^{1}H-^{13}C bond correlations which help resolve overlapping signals from ^{1}H NMR data [*Simpson*, 2001]. Figure 7 shows the HMQC NMR spectrum of an alkaline extract from inside the pockmark at 6 mbsf. The *N*-acetyl functional group from peptidoglycan is prominent in this and all HMQC NMR spectra from all depths inside and outside the pockmark. Peptidoglycan is a polymer that consists of sugars and amino acids that forms a layer outside the plasma membrane of bacteria. It has been used to estimate bacterial concentrations [*Benner and Kaiser*, 2003; *Simpson et al.*, 2007b] and can be protected from microbial degradation after cell death by copolymerization reactions and transformation, substantially adding to the refractory nitrogen pool [*Benner and Kaiser*, 2003; *Loll and Bollag*, 1983]. Muramic acid is only found in peptidoglycan, where it is linked to both a glycan strand and peptide side chain. Gram-positive cells contain 5- to 10-fold greater yields of muramic acid than Gram-negative cells [*Moriarty*, 1977; *Benner and Kaiser*, 2003]. However, most bacteria in seawater and marine sediments are Gram-negative [*Moriarty and Hayward* 1982; *Giovannoni and Rappe*, 2000] including methanotrophic bacteria. Archaea do not contain muramic acid in their cell walls [*Brock et al.*, 1994] and as yet an NMR indicator or signal that allows us to differentiate between bacteria and Archaea has not been reported. Archaea comprise about half of the total direct count of cells in deep water [*Karner et al.* 2001] and therefore archaeal residue is likely to be present in the organic extracts. From the NMR data reported here, we can say that both living and non-living Gram-positive and -negative cells are strongly contributing to the sedimentary organic matter. The peptidoglycan signature is very significant at all depths inside and outside the pockmark.

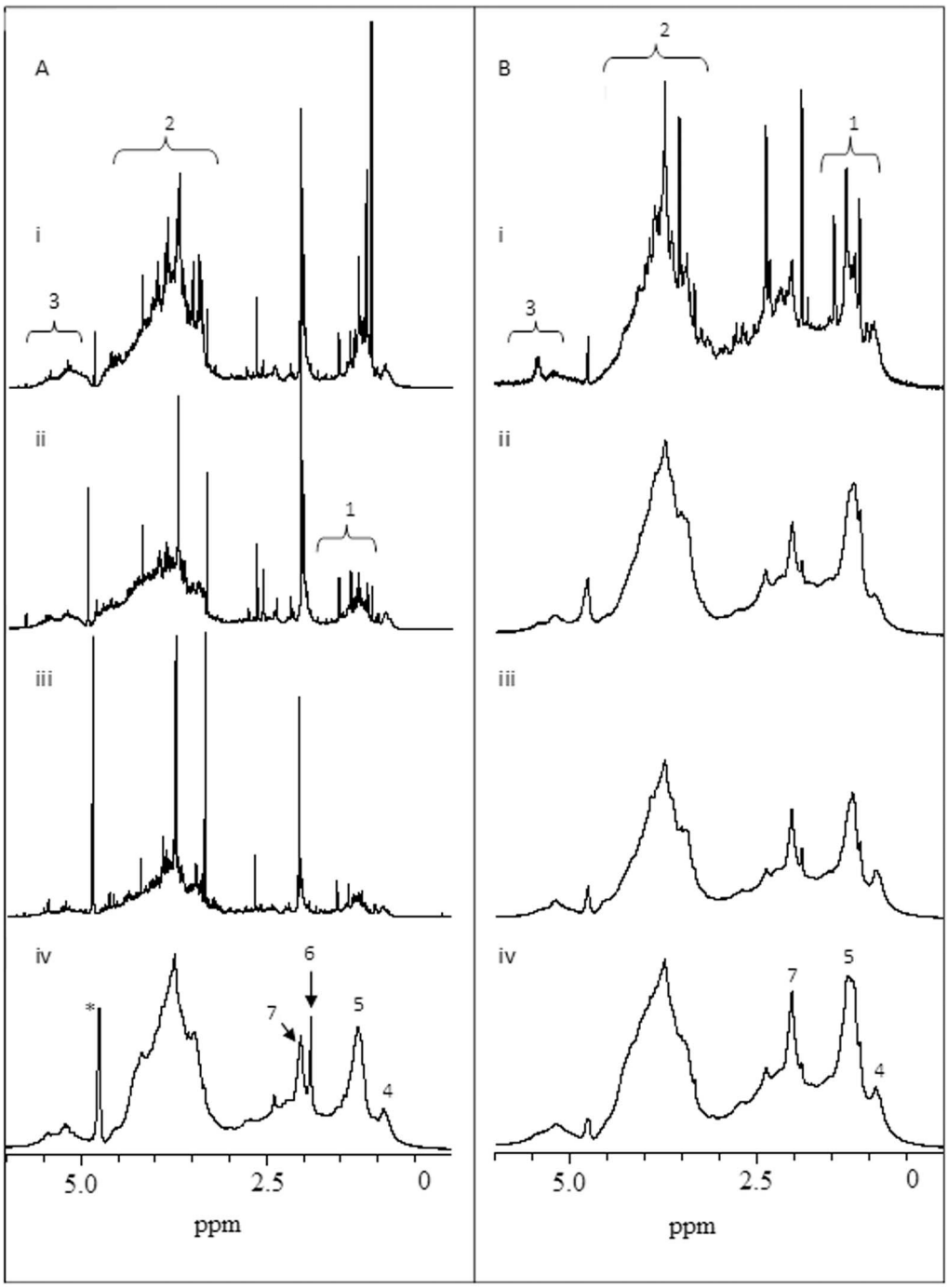

Figure 6. 1D ^{1}H NMR spectra (0–6 ppm) of sediment profiles from (a) outside and (b) inside the pockmark. (i) Surface, (ii) 2 mbsf, (iii) 4 mbsf and (iv) 6 mbsf. Designations 1–3 indicate general spectral regions: (1) aliphatics; (2) carbohydrates and amino acids (*O*-alkyl) and (3) anomeric carbon. Designations 4–7 indicate specific assignments: (4) aliphatic CH_3; (5) aliphatic methylene $(CH_2)_n$; (6) acetic acid; (7) peptidoglycan. Residual water.

[29] To further emphasize the strong signature from microbial biomass, diffusion edited (DE) NMR was performed. In diffusion edited NMR experiments, small molecules are essentially gated from the final spectrum but signals from macromolecules and/or rigid domains (for example cellular structures) which display little translational diffusion are not gated and appear in the spectrum [*Wu et al.*, 1995]. The diffusion edited spectra of the four depths from both cores are shown in Figure 8. The presence of

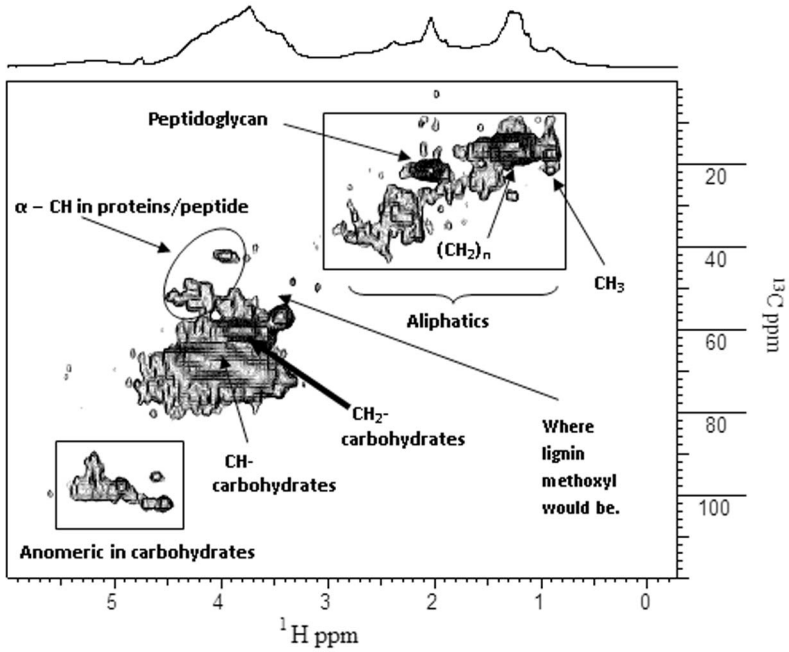

Figure 7. Zoom region of ^{1}H-^{13}C HMQC for sediment extract from inside the pockmark (6 mbsf). The lack of a strong resonance in the methoxyl region indicates that lignin is not a major component of the samples studied here.

aliphatic chains and carbohydrates suggests that they exist in rigid domains or are macromolecular in structure. Peptidoglycan is macromolecular and its resonance peak is extremely strong in all spectra but particularly so outside the pockmark. The organic matter outside the pockmark is dominated by microbial biomass and there is less organic matter obvious from other sources. This is particularly evident when comparing the relative intensities of the peptidoglycan peaks to those in the aliphatic region of the spectra. The microbial signature is not as strong relative to other carbon such as carbohydrates and lipids in the first three depths inside the core. The organic matter from the outside core appears to be strongly associated with bacteria while much of the organic matter inside the core may come from other sources. While there are clear differences in the top three depths between the cores, the DE spectra for the lowest depth (6 m) are again similar. Further evidence of the dominance of microbial biomass is provided by the clear contribution from α-CH units in Figure 7 that give a very characteristic group of resonances in H-C 2D NMR [*Simpson et al.*, 2007a]. α-CH groups are likely from microbial peptides/proteins and vertical elongation of the CH_3 band indicates that protein side chains also resonate here [*Simpson et al.*, 2007a, 2007b].

[30] Sharp resonances in Figures 6 and 9 are consistent with small molecules which can be related to microbial activity in environmental samples [*Simpson et al.*, 2011]. Metabolic activity of microbes is evident on the surface sediment of both cores and is consistent down the outside core profile apart from the deepest sample. However, signs of activity are only detectable on the surface of the inside core and not observed down core suggesting that the activity within the pockmark is considerably decreased. Signatures of microbial activity differ on the surface of both cores indicating that microbial communities may not be the same. Despite the lack of activity within the inside core, there are still strong peptidoglycan signals and an accumulation of aliphatic structures (e.g., lipids). In this case, the microbial signatures may be derived from the cell walls of non-living microbes that are degrading or dormant microbes that are less active than their counterparts from outside the pockmark. This is consistent with the diffusion editing data (Figure 8), which show microbial signatures in abundance and organic matter from other sources (i.e., potential food sources) depleted outside the pockmark relative to inside. This suggests the microbes outside the pockmark are utilizing the organic matter and thus are active, whereas the microbes inside the pockmark are less active as other sources of organic matter have accumulated.

[31] Also prominent in the 2D spectra (Figure 7) are CH and CH_2 functionalities originating from carbohydrates. All spectra are dominated by carbohydrate resonances. Carbohydrate is presumed to be

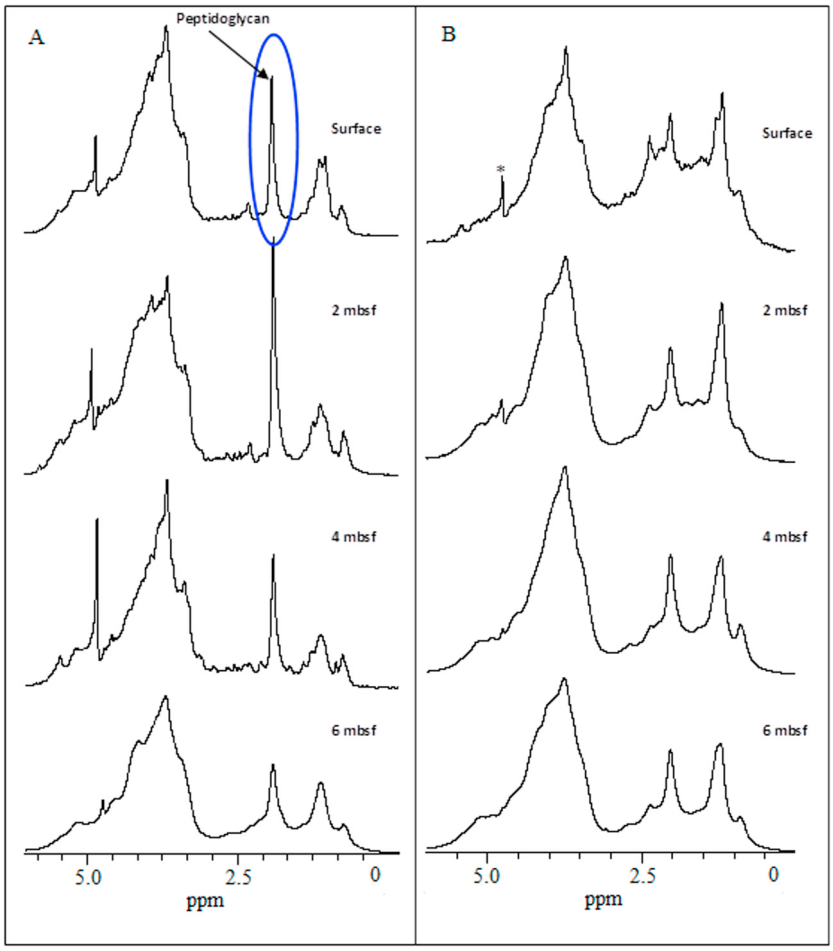

Figure 8. DE ^{1}H NMR of sediment cores from (a) inside and (b) outside the pockmark. Profound peptidoglycan signals are found in the reference core indicating increased microbial presence.

relatively reactive in the marine environment and its presence is likely due to a combination of newly synthesized structures and/or labile structure catabolism into the more stable alkyl fractions [*Baldock et al.*, 1990]. Remineralized carbohydrate may become more recalcitrant through interactions with biopolymers such as lignin. Lignin presence would indicate a terrestrial influence but there are no clear indicators of the presence of lignin in abundance either in the 1 or 2D experiments (Figures 6 and 7), indicating that in this case, the high concentrations of carbohydrate do not rely on this mechanism for survival [*Kelleher and Simpson*, 2006; *Simpson et al.*, 2004]. Again, a large portion of carbohydrates are likely derived from dead and living marine microbial cells [*Simpson et al.*, 2007a]. In addition, it has been reported that *O*-alkyl and acetyl carbon (anomeric carbon constituents) can serve as substrates for bacteria in sediment organic matter and increased microbial activity can result in the synthesis of new carbohydrates, initially increasing the labile SOM concentration [*Sjögersten et al.*, 2003]. Over time, the catabolism of *O*-alkyl carbon by microbes leads to a net alkyl carbon accumulation by the synthesis of new alkyl carbon structures which may help explain some of the alkyl carbon observed at the lowest depth outside and at 2, 4 and 6 mbsf inside the pockmark [*Baldock et al.*, 1990].

4. Conclusions

[32] Gas related acoustic signatures were recorded in the sub-bottom profiles of a large composite pockmark on the Malin Shelf, Ireland. Sub-bottom profiles reveal a relatively large gas pocket approximately 20 m underneath the pockmark feature, subtle fluid flow vertical signatures and indicators of lateral gas accumulation in the near-seabed subsurface. Despite an abundance of these subsurface gas related signals there was no evidence of seepage to the water column during data acquisition.

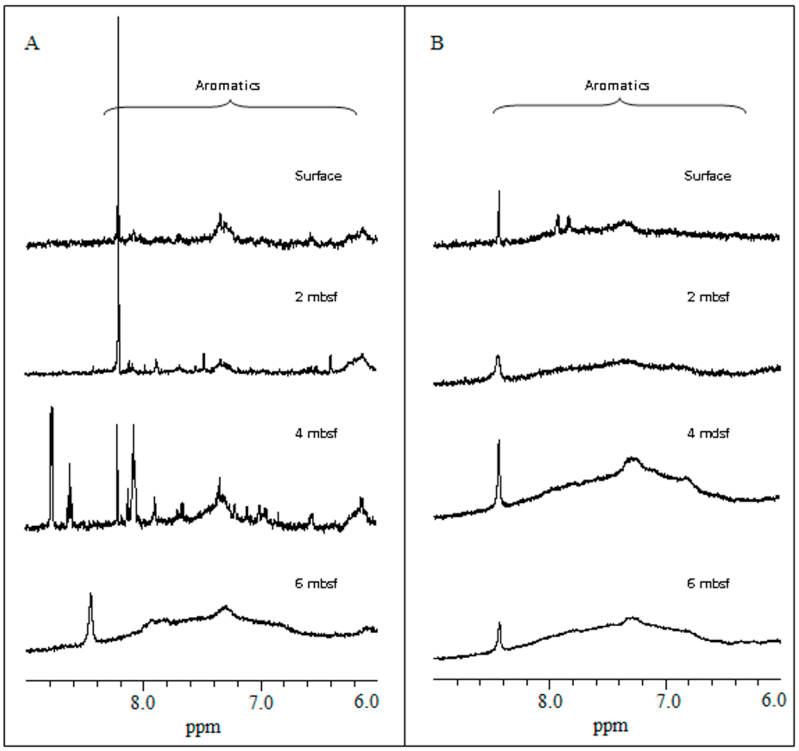

Figure 9. 1D ^{1}H NMR (6–9 ppm) spectra of sediment profiles from (a) outside and (b) inside the pockmark showing aromatic signal distribution in the sediment.

However, an active fluid system is present and fluid is migrating within the sedimentary body. The subsurface directly beneath the pockmark (up to 3 m below seafloor) remains structureless, without obvious layering exhibited in the surroundings, suggesting that sediment has been mixed, possibly during pockmark formation. The surrounding sediments, including those around the reference core show narrowly spaced parallel layering and no obvious structural signs of fluid flow disruption.

[33] Electrical conductivity profiles within the pockmark show anomalous lows attributed to the presence of gas. However, several sharp high conductivity peaks underneath the pockmark and its vicinity are present. One of these peaks (A, Figure 4) can be correlated to high levels of peptidoglycan in the sediment core (VC044). This relationship may be attributed to increased bacterial presence or presence of bacterial necromass. Higher conductivity levels on the edges of the pockmarks (S1 and S2) may have been caused by similar processes or by disruption of sediment structure possibly by fluid displacement.

[34] Sulphate profiles from both sediment cores indicate a recent upward movement of gas. The methane flux is higher underneath the pockmark than in the reference site suggesting that the main migration pathway is partially active and connected to the main gas accumulation reservoir underneath. As a result the SMTZ of the reference core is slightly deeper than the pockmark core. The deeper SMTZ of the reference core may also partially explain the abundance of microbial signatures in the organic matter down the reference core. However, it does not explain the paucity of these signatures inside the pockmark as suggested by NMR data. The decreased microbial activity within the pockmark may be linked to less available methane within the first meters of sediment as suggested by the presence of reworked sediment. Analysis of the organic matter by NMR shows that the cellular contents from previous generations of microbes (including lipids) are accumulating as they are not used up quickly. Outside however lateral gas bearing bodies can provide an additional carbon source for microbes and the observed high activity is likely facilitated by access to this source.

Acknowledgments

[35] We wish to thank the Geological Survey of Ireland, the **IN**tegrated Mapping **FO**r the Sustainable Development of

Ireland's **MA**rine **R**esource (INFOMAR) program, the Irish Environmental Protection Agency, Science Foundation of Ireland, QUESTOR (Queens University Belfast) and the Irish Council for Science, engineering and technology for funding this research. AJS thanks NSERC, (Strategic and Discovery Programs), the Canada Foundation for Innovation (CFI), and the Ministry of Research and Innovation (MRI) for providing Canadian funding. The survey data utilized in the research has been co-funded by the Geological Survey of Ireland and the Offshore Irish Petroleum Infrastructure Programme (PIP; Ref. No: IS05/16 Malin Basin EM). We finally thank Øyvind Hammer and Kris Hart whose comments greatly improved the paper.

References

Abdel Aal, G. Z., E. A. Atekwana, and E. A. Atekwana (2010a), Effect of bioclogging in porous media on complex conductivity signatures, *J. Geophys. Res.*, *115*, G00G07, doi:10.1029/2009JG001159.

Abdel Aal, G. Z., E. A. Atekwana, S. Rossbach, and D. D. Werkema (2010b), Sensitivity of geoelectrical measurements to the presence of bacteria in porous media, *J. Geophys. Res.*, *115*, G03017, doi:10.1029/2009JG001279.

Allen, J. P., E. A. Atekwana, E. A. Atekwana, J. W. Duris, D. D. Werkema, and S. Rossbach (2007), The microbial community structure in petroleum-contaminated sediments corresponds to geophysical signatures, *Appl. Environ. Microbiol.*, *73*, 2860–2870, doi:10.1128/AEM.01752-06.

Atekwana, E. A., D. D. Werkema Jr., J. W. Duris, S. Rossbach, E. A. Atekwana, W. A. Sauck, D. P. Cassidy, J. Means, and F. D. Legall (2004), *In-situ* apparent conductivity measurements and microbial population distribution at a hydrocarbon-contaminated site, *Geophysics*, *69*, 56–63, doi:10.1190/1.1649375.

Baldock, J. A., J. M. Oades, A. M. Vassallo, and M. A. Wilson (1990), Significance of microbial activity in soils as demonstrated by solid-state ^{13}CNMR, *Environ. Sci. Technol.*, *24*(4), 527–530, doi:10.1021/es00074a010.

Benner, R., and K. Kaiser (2003), Abundance of amino sugars and peptidoglycan in marine particulate and dissolved organic matter, *Limnol. Oceanogr.*, *48*(1), 118–128, doi:10.4319/lo.2003.48.1.0118.

Berkson, J. M., and C. S. Clay (1973), Possible syneresis marine seismic study of late Quaternary sedimentation origin of valleys on the floor of Lake Superior, *Nature*, *245*, 89–91, doi:10.1038/245089a0.

Blott, S. J., and K. Pye (2001), GRADISTAT: A grain size distribution and statistics package for the analysis of unconsolidated sediments, *Earth Surf. Processes Landforms*, *26*, 1237–1248, doi:10.1002/esp.261.

Bøe, R., L. Rise, and D. Ottesen (1998), Elongate depressions on the southern slope of the Norwegian Trench (Skagerrak): Morphology and evolution, *Mar. Geol.*, *146*, 191–203, doi:10.1016/S0025-3227(97)00133-3.

Boetius, A., K. Ravenschlag, C. J. Schubert, D. Rickert, F. Widdel, A. Gieseke, R. Amann, B. B. Jørgensen, U. Witte, and O. Pfannkuche (2000), A marine microbial consortium apparently mediating anaerobic oxidation of methane, *Nature*, *407*, 623–626, doi:10.1038/35036572.

Borowski, W. S., C. K. Paull, and W. I. I. I. Ussler (1996), Marine pore water sulfate profiles indicate in situ methane flux from underlying gas hydrate, *Geology*, *24*, 655–658, doi:10.1130/0091-7613(1996)024<0655:MPWSPI>2.3.CO;2.

Boudreau, B. P. (1997), *Diagenetic Models and Their Implementation: Modeling Transport and Reactions in Aquatic Sediments*, Springer, Berlin.

Brock, T. D., M. T. Madigan, J. M. Martinko, and J. Parker (1994), *Biology of Microorganisms*, 7th ed., Prentice Hall, Englewood Cliffs, N. J.

Cathles, L. M., Z. Su, and D. Chen (2010), The physics of gas chimney and pockmark formation, with implications for assessment of seafloor hazards and gas sequestration, *Mar. Pet. Geol.*, *27*, 82–91, doi:10.1016/j.marpetgeo.2009.09.010.

Cheesman, S. J. (1989), A short baseline transient electromagnetic method for use on the sea floor, PhD thesis, 138 pp., Univ. of Toronto, Toronto, Ontario, Canada.

Christodoulou, D., G. Papatheodorou, G. Ferentinos, and M. Masson (2003), Active seepage in two contrasting pockmark fields in the Patras and Corinth gulfs, Greece, *Geo Mar. Lett.*, *23*, 194–199, doi:10.1007/s00367-003-0151-0.

Dando, P. R., M. C. Austen, R. A. Burke Jr., M. A. Kendall, M. C. Kennicutt II, A. G. Judd, D. C. Moore, S. C. M. O'Hara, R. Schmaljohann, and A. J. Southward (1991), Ecology of a North Sea pockmark with an active methane seep, *Mar. Ecol. Prog. Ser.*, *70*, 49–63, doi:10.3354/meps070049.

Dobson, M. R., and R. J. Whittington (1992), Aspects of the geology of the Malin Sea area, in *Basins on the Atlantic Seaboard: Petroleum Geology, Sedimentology and Basin Evolution*, edited by J. Parnell, *Geol. Soc. Spec. Publ.*, *62*, 291–311.

Dorschel, B., A. J. Wheeler, X. Monteys, and K. Verbruggen (2010), *Atlas of the Deep-Water Ireland*, 161 pp., Springer, Dordrecht, Netherlands, doi:10.1007/978-90-481-9376-9.

Dunlop, P., R. Shannon, M. McCabe, R. Quinn, and E. Doyle (2010), Marine geophysical evidence for ice sheet extension and recession on the Malin Shelf: New evidence for the western limits of the British Irish Ice Sheet, *Mar. Geol.*, *276*, 86–99, doi:10.1016/j.margeo.2010.07.010.

Ellis, M., R. L. Evans, D. Hutchinson, P. Hart, J. Gardner, and R. Hagen (2008), Electromagnetic surveying of seafloor mounds in the Northern Gulf of Mexico, *Mar. Pet. Geol.*, *25*, 960–968, doi:10.1016/j.marpetgeo.2007.12.006.

Evans, D., R. J. Whittington, and M. R. Dobson (1986), Tiree, in *British Geological Survey 1:250,000 Series: Solid Geology*, sheet 56°N 08°W, Br. Geol. Surv., Keyworth, U. K.

Evans, R. L. (2007), Using CSEM techniques to map the shallow section of seafloor: From the coastline to the edges of the continental slope, *Geophysics*, *72*, WA105–WA116, doi:10.1190/1.2434798.

Fader, G. B. J. (1991), Gas-related sedimentary features from the eastern Canadian continental shelf, *Cont. Shelf Res.*, *11*, 1123–1153, doi:10.1016/0278-4343(91)90094-M.

Ferdelman, T. G., H. Fossing, K. Neumann, and H. D. Schulz (1999), Sulphate reduction in surface sediments of the Southeast Atlantic continental margin between 15°38′S and 27°57′S (Angola and Namibia), *Limnol. Oceanogr.*, *44*(3), 650–661, doi:10.4319/lo.1999.44.3.0650.

Fossing, H., T. G. Ferdelman, and P. Berg (2000), Sulphate reduction and methane oxidation in continental margin sediments influenced by irrigation (South-East Atlantic off Namibia), *Geochim. Cosmochim. Acta*, *64*, 897–910, doi:10.1016/S0016-7037(99)00349-X.

Garcia, X., X. Monteys, R. Evans, and B. Kelleher (2007), Geohazard identification and early reconnaissance for hydro-

carbon potential using marine electromagnetic and high frequency acoustic methods, *Geophys. Res. Abstr.*, *9*, 09524.
Gélinas, Y., J. A. Baldock, and J. I. Hedges (2001), Demineralization of marine and freshwater sediments for CP/MAS ^{13}C NMR analysis, *Org. Geochem.*, *32*(5), 677–693, doi:10.1016/S0146-6380(01)00018-3.
Giovannoni, S., and M. Rappe (2000), Evolution, diversity, and molecular ecology of marine prokaryotes, in *Microbal Ecology of the Oceans*, edited by D. L. Kirchman, pp. 47–84, Wiley, New York.
Gonçalves, C. N., R. S. D. Dick, D. P. Dalmolin, H. Knicker, E. Klamt, and I. Kogel-Knabner (2003), The effect of 10% HF treatment on the resolution of CPMAS ^{13}C NMR spectra and on the quality of organic matter in Ferralsols, *Geoderma*, *116*(3–4), 373–392, doi:10.1016/S0016-7061(03)00119-8.
Gowen, R. J., R. Raine, M. Dickey-Collas, and M. White (1998), Plankton distribution in relation to physical oceanographic features on the southern Malin Shelf, August 1996, *ICES J. Mar. Sci.*, *55*, 1095–1111, doi:10.1006/jmsc.1998.0418.
Hay, A. E. (1984), Remote acoustic imaging of the plume from a submarine spring in an arctic fjord, *Science*, *225*, 1154–1156, doi:10.1126/science.225.4667.1154.
Hensen, C., M. Zabel, K. Pfeifer, T. Schwenk, S. Kasten, N. Reidinger, H. D. Schulz, and A. Boetius (2003), Control of sulfate pore-water profiles by sedimentary events and the significance of anaerobic oxidation of methane for the burial of sulfur in marine sediments, *Geochim. Cosmochim. Acta*, *67*, 2631–2647, doi:10.1016/S0016-7037(03)00199-6.
Hovland, M., and A. G. Judd (1988), *Seabed Pockmarks and Seepages: Impact on Geology, Biology and Marine Environment*, Graham and Trotman, London.
Hovland, M., et al. (1997), Gas hydrate and free gas volumes in marine sediments: Example from the Niger Delta front, *Mar. Pet. Geol.*, *14*, 245–255, doi:10.1016/S0264-8172(97)00012-3.
Hovland, M., R. Heggland, M. H. De Vries, and T. I. Tjelta (2010), Unit-pockmarks and their potential significance for predicting fluid flow, *Mar. Pet. Geol.*, *27*, 1190–1199, doi:10.1016/j.marpetgeo.2010.02.005.
Judd, A. G., and M. Hovland (2007), *Seabed Fluid Flow: The Impact on Geology, Biology, and the Marine Environment*, Cambridge Univ. Press, Cambridge, U. K., doi:10.1017/CBO9780511535918.
Karner, M. B., E. F. Delong, and D. M. Karl (2001), Archaeal dominance in the mesopelagic zone of the Pacific Ocean, *Nature*, *409*, 507–510, doi:10.1038/35054051.
Kelleher, B. P., and A. J. Simpson (2006), Humic substances in soils: Are they really chemically distinct?, *Environ. Sci. Technol.*, *40*(15), 4605–4611, doi:10.1021/es0608085.
Kelley, J. T., et al. (1994), Giant seabed pockmarks: Evidence for gas escape from Belfast Bay, *Mar. Geol.*, *22*, 59–62, doi:10.1130/0091-7613(1994)022<0059:GSBPEF>2.3.CO;2.
Khilyuk, L. F., G. V. Chilingar, J. O. Robertson Jr., and B. Endres (2000), *Gas Migration: Events Preceding Earthquakes*, Gulf Publ. Co., Houston, Tex.
Loll, M. J., and J. M. Bollag (1983), Protein transformation in soil, *Adv. Agron.*, *36*, 351–382, doi:10.1016/S0065-2113(08)60358-2.
MacDonald, I. R., N. L. Guinasso Jr., R. Sassen, J. M. Brooks, L. Lee, and K. T. Scott (1994), Gas hydrate that breaches the sea floor on continental slope of the Gulf of Mexico, *Geology*, *22*, 699–702, doi:10.1130/0091-7613(1994)022<0699:GHTBTS>2.3.CO;2.
Monteys, X., D. Hardy, E. Doyle, and S. Garcia-Gil (2008a), Distribution, morphology and acoustic characterisation of a gas pockmark field on the Malin Shelf, NW Ireland, paper presented at 33rd International Geological Congress, Symposium OSP-01, Int. Union of Geol. Sci., Oslo.
Monteys, X., X. Garcia, M. Szpak, S. Garcia-Gil, B. Kelleher, and E. O'Keffee (2008b), Multidisciplinary approach to the study and environmental implications of two large pockmarks on the Malin Shelf, Ireland, paper presented at Ninth International Conference on Gas in Marine Sediments, Univ. Bremen, Bremen, Germany.
Moriarty, D. J. W. (1977), Improved method using muramic acid to estimate biomass of bacteria in sediments, *Oecologia*, *26*, 317–323, doi:10.1007/BF00345531.
Moriarty, D., and A. C. Hayward (1982), Ultrastructure of bacteria and the proportion of Gram-negative bacteria in marine sediments, *Microb. Ecol.*, *8*, 1–14, doi:10.1007/BF02011456.
Niewöhner, C., C. Hensen, S. Kasten, M. Zabel, and H. D. Schulz (1998), Deep sulfate reduction completely mediated by anaerobic methane oxidation in sediments of the upwelling area off Namibia, *Geochim. Cosmochim. Acta*, *62*, 455–464, doi:10.1016/S0016-7037(98)00055-6.
Pake, G. E., and T. L. Estle (1973), *The Physical Principles of Electron Paramagnetic Resonance*, *Front. Phys.*, 2nd ed., W. A. Benjamin, Reading, Mass.
Parnell, J. (1992), Burial histories and hydrocarbon source rocks on the North West Seaboard, in *Basins on the Atlantic Seaboard: Petroleum Geology, Sedimentology and Basin Evolution*, edited by J. Parnell, *Geol. Soc. Spec. Publ.*, *62*, 3–16, doi:10.1144/GSL.SP.1992.062.01.02.
Pilcher, R., and J. Argent (2007), Mega-pockmarks and linear pockmark trains on the West African continental margin, *Mar. Geol.*, *244*, 15–32, doi:10.1016/j.margeo.2007.05.002.
Pimenov, N. V., A. S. Savvichev, I. I. Rusanov, A. Y. Lein, and M. V. Ivanov (2000), Microbiological processes of the carbon and sulfur cycles at cold methane seeps of the North Atlantic, *Microbiology*, *69*, 709–720, doi:10.1023/A:1026666527034.
Riddihough, R. P. (1968), Magnetic surveys off the north coast of Ireland, *Proc. R. Ir. Acad., Sect. B*, *66*, 27–41.
Schulz, H. D., and M. Zabel (Eds.) (2006), *Marine Geochemistry*, 2nd ed., Springer, Berlin, doi:10.1007/3-540-32144-6.
Schulz, H. D., A. Dahmke, U. Schinzel, K. Wallmann, and M. Zabel (1994), Early diagenetic processes, fluxes, and reaction rates in sediments of the South Atlantic, *Geochim. Cosmochim. Acta*, *58*, 2041–2060, doi:10.1016/0016-7037(94)90284-4.
Simpson, A. (2001), Multidimensional solution state NMR of humic substances: A practical guide and review, *Soil Sci.*, *166*(11), 795–809, doi:10.1097/00010694-200111000-00006.
Simpson, A. J., and S. A. Brown (2005), PURGE NMR: Effective and easy solvent suppression, *J. Magn. Reson.*, *175*, 340–346, doi:10.1016/j.jmr.2005.05.008.
Simpson, A. J., W. L. Kingery, A. Williams, S. Golotvin, M. Kvasha, B. P. Kelleher, A. Moser, and B. Lefebvre (2004), Identifying residues in natural organic matter through spectral prediction and pattern matching of 2-D NMR datasets, *Magn. Reson. Chem.*, *42*(1), 14–22, doi:10.1002/mrc.1308.
Simpson, A. J., W. L. Kingery, M. J. Simpson, and B. P. Kelleher (2006), The Application of ^{1}H high resolution magic angle spinning NMR to the study of clay-organic

associations in synthetic complexes, *Langmuir*, *22*(10), 4498–4503, doi:10.1021/la052679w.

Simpson, A. J., M. J. Simpson, E. Smith, and B. P. Kelleher (2007a), Microbially derived inputs to soil organic matter: Are current estimates too low?, *Environ. Sci. Technol.*, *41*(23), 8070–8076, doi:10.1021/es071217x.

Simpson, A. J., G. X. Song, E. Smith, B. Lam, E. H. Novotny, and M. H. B. Hayes (2007b), Unraveling the structural components of soil humin by use of solution-state nuclear magnetic resonance spectroscopy, *Environ. Sci. Technol.*, *41*(3), 876–883, doi:10.1021/es061576c.

Simpson, A. J., D. McNally, and M. J. Simpson (2011), NMR spectroscopy in environmental research: From molecular interactions to global processes, *Prog. Nucl. Magn. Reson. Spectrosc.*, *58*, 97–175, doi:10.1016/j.pnmrs.2010.09.001.

Sjögersten, S., B. L. Turner, N. Mahieu, L. M. Condron, and P. A. Wookey (2003), Soil organic matter biochemistry and potential susceptibility to climatic change across the forest-tundra ecotone in the Fennoscandian mountains, *Global Change Biol.*, *9*(5), 759–772, doi:10.1046/j.1365-2486.2003.00598.x.

Stein, R. (1990), Organic carbon content/sedimentation rate relationship and its paleoenvironmental significance for marine sediments, *Geo Mar. Lett.*, *10*, 37–44, doi:10.1007/BF02431020.

Stoker, M. S. (1981), Pockmark morphology: A preliminary description; Evidence for slumping and doming, *Rep. 81/10*, Inst. of Geol. Sci., Edinburgh, U. K.

Wu, D. H., A. D. Chen, and C. S. Johnson (1995), An improved diffusion ordered spectroscopy experiment incorporating bipolar-gradient pulses, *J. Magn. Reson., Ser. A*, *115*, 260–264, doi:10.1006/jmra.1995.1176.

Zabel, M., and H. D. Schulz (2001), Importance of submarine landslides for non-steady state conditions in pore-water systems–Lower Zaire (Congo) deep-sea fan, *Mar. Geol.*, *176*, 87–99, doi:10.1016/S0025-3227(01)00164-5.